2021

Assessment of Metal-Hydride Energy Storage Coupled with Heat Pumps and Solar PV for Residential Cooling and Heating

Patrick Krane
Purdue University, United States of America, pkrane@purdue.edu

Davide Ziviani
Purdue University, United States of America

James E. Braun
Purdue University, United States of America

Neera Jain
Purdue University, United States of America

Amy Marconnet
Purdue University, United States of America

Assessment of Metal-Hydride Energy Storage Coupled with Heat Pumps and Solar PV for Residential Cooling and Heating

Patrick KRANE[1], Davide ZIVIANI[1], James E BRAUN[1], Neera JAIN[1], Amy MARCONNET[1,*]

[1]School of Mechanical Engineering, Purdue University,
West Lafayette, IN 47907
Contact Information (marconnet@purdue.edu)

* Corresponding Author

ABSTRACT

The extension of time-of-use (TOU) rates to residential buildings has incentivized the use of thermal energy storage (TES) to shift heating and cooling loads away from on-peak hours. At the same time, the growing use of solar photovoltaics (PV) for on-site energy generation with variable buy back rates also encourages the use of TES to store energy generated at hours of peak solar radiation. Metal hydrides are reversible chemical compounds that form when certain metals react with hydrogen. Since these reactions depend on both temperature and pressure, metal hydrides can be used for thermochemical energy storage across a range of temperatures. Because of this, metal hydrides can be used as storage for both heating and cooling, enabling year-round utilization. In this paper, we present and evaluate a system that combines metal hydride energy storage with heat pumps and on-site PV. The system is designed to reduce operating costs by discharging the energy storage system during on-peak hours when electricity is expensive and charging the system during off-peak periods when electricity is less expensive and there is less incentive to sell excess PV electricity generation back to the grid. The TOU rates considered are designed for a future scenario with high solar penetration, where greater solar generation in the afternoon leads to on-peak periods in the mornings and evenings rather than the afternoon. The payback period of the energy storage system is estimated using energy savings relative to a baseline of a solar home without an energy storage system along with estimates of additional installed costs for the storage system. Payback period calculations for a range of rates show that rates with on-peak demand charges result in larger cost savings than rates with high on-peak rates, but even for the most favorable rates, the payback period is too long for the system to be economically viable.

1. INTRODUCTION

In recent years, it has become more common for time-of-use (TOU) utility rate structures to be available as an option for residential buildings. Time-of-use rates are used to incentivize consumers to use less electricity at times when demand for electricity from the grid is highest (on-peak hours). One way of doing this is by using energy storage to shift some of the building's heating or cooling load from on-peak hours to off-peak hours. This involves charging the storage system during off-peak hours and discharging during on-peak hours. In commercial buildings, where TOU rate structures have been in use for a longer time, ice storage is often used for this purpose. In this case, a chiller is used to freeze ice during off-peak hours and then the ice is melted during on-peak hours to deliver a portion of the cooling load (Hasnain, 1998; Henze, 2003; Nassif *et al.*, 2013; Sanaye & Shirazi, 2013; Tam *et al.*, 2019). Ice storage has been studied for use in residential buildings. However, it was found to have too large a payback period to be economic in most cases with best economic potential in locations with long cooling seasons (Tam *et al.*, 2018).

The cost savings from energy storage could potentially be increased if an energy storage system were capable of being used year-round for both heating and cooling (as compared to ice storage, which is only used for cooling). One way to accomplish this is to use metal hydrides for thermochemical energy storage. Metal hydrides are metals that exothermically adsorb hydrogen if the hydrogen pressure is greater than the equilibrium pressure for the adsorption reaction, and endothermically desorb hydrogen if the pressure is below equilibrium. The equilibrium pressures for these reactions are a function of the temperature and the hydrogen absorbed by the metal hydride (Voskuilen *et al.*, 2014). Because of this, the temperature at which the reaction occurs can be altered by adjusting the hydrogen pressure around the hydride. This makes metal hydride suitable for use in an energy storage system designed for both heating and cooling.

Previous work on using metal hydrides for energy storage has primarily focused on storage for concentrated solar power, due to the potential of certain metal hydrides for use in high-temperature applications (Corgnale *et al.*, 2016; Feng *et al.*, 2018; Nyamsi *et al.*, 2018; Sheppard *et al.*, 2016). A common system design for energy storage is to have two metal hydride reactors, one of which is used to store and release energy through the adsorption and desorption reactions, while the other is used to store the hydrogen released by the other reactor and release it back to it (Corgnale *et al.*, 2016; Nyamsi *et al.*, 2018; Sheppard *et al.*, 2016; Ward *et al.*, 2016).

The increasing use of solar photovoltaics (PV) for on-site energy generation provides additional benefits for the use of energy storage in load shifting for both cooling and heating. Available solar power in the afternoon significantly reduces demand from the grid during on-peak hours (VanGeet *et al.*, 2008). With sufficient solar penetration, peak electricity demand from the grid would no longer occur in the afternoon but in the morning and evening (Janko *et al.*, 2016). However, there is a significant mismatch between peak solar generation (around noon) and peak power demand (around 5 PM). A study of solar power in Wisconsin found that this results in diminishing returns for solar penetration once it accounts for 15-20% of power generation, but that solar penetration could be significantly increased if the demand curve were shifted to be closer to the solar generation curve (Myers *et al.*, 2010). Energy storage could be used to accomplish this, and the shifting of peak demand from the grid to the morning and evening would incentivize utility companies to charge TOU rates that would encourage shifting loads away from these times.

Rate structures for locations that have significant on-site generation typically include an avoided cost rate (ACR), which is a credit given for times when on-site generation exceeds consumption. The ACR is generally significantly lower than the rate charged for electricity usage (Leger *et al.*, 2014), which provides an incentive for using on-site PV to charge a storage system when generation exceeds consumption. Previous studies have adjusted discharge rates for storage during on-peak hours based on whether solar generation exceeds demand (Abji *et al.*, 2015). The current paper also considers a load-shifting strategy that adjusts the charging rate based on available solar power in combination with the use of metal hydride storage for both cooling and heating with a heat pump.

In this paper, we model a two-reactor metal hydride energy storage system coupled with on-site solar PV generation and examine its performance in a residential building for a full year of operation. We estimate the operating cost savings and payback period of this system using utility rate structures designed for a location with increased solar penetration.

2. METHODOLOGY

2.1 System Model

A diagram of the model used for evaluating the performance of the metal hydride energy storage system and determining its annual operating cost can be seen in Figure 1. This model combines a static model of the heat pump and secondary loops with a dynamic model of the metal hydride reactors. A schematic of the system is shown in Figure 1. A heat pump is used to provide the heating and cooling loads to the house, with a water glycol loop used to deliver this load from the heat pump to the house. This heat pump is connected to two water glycol loops: an *indoor loop*, which exchanges heat with an indoor unit in the house as well as the heat pump, and an *outdoor loop*, which exchanges heat with an external heat exchanger as well as the heat pump. A 4-way valve is used to reverse which loop the heat pump transfers heat to and which it removes heat from. Each water glycol loop can also be used to exchange heat with either of the metal hydride reactors. In cooling mode, the low-temperature reactor is connected to the indoor loop, and the high-temperature reactor to the outdoor loop. The system is charged by using the heat transferred from the heat pump to the outdoor loop to heat the high-temperature reactor, causing the metal hydride there to desorb hydrogen, which then flows to the low-temperature reactor. This reactor absorbs hydrogen, releasing heat into the indoor loop. The system is discharged by sending water glycol from the outdoor loop to the hydride reactor after the water glycol has been cooled by the external unit instead of after it has been heated by the heat pump. This lower temperature lowers the equilibrium pressure in the reactor, resulting in hydrogen flow from the low-temperature reactor to the high-temperature reactor, which results in the low-temperature reactor desorbing hydrogen that is absorbed by the high-temperature reactor. These reactions result in the high-temperature reactor releasing heat while the low-temperature reactor absorbs heat from the water glycol in the indoor loop, thus cooling it and providing a portion of the cooling load for the house. In both charging and discharging, if the change in temperature is not enough to drive the reaction and hydrogen flow, a compressor is used to drive hydrogen flow between the reactors. In heating mode, the same reactions occur in the reactors in charging and discharging, but which reactor is connected to which

water glycol loop changes. Thus, the high-temperature reactor is connected to the indoor loop and absorbs heat from it while charging and releases heat to it while discharging.

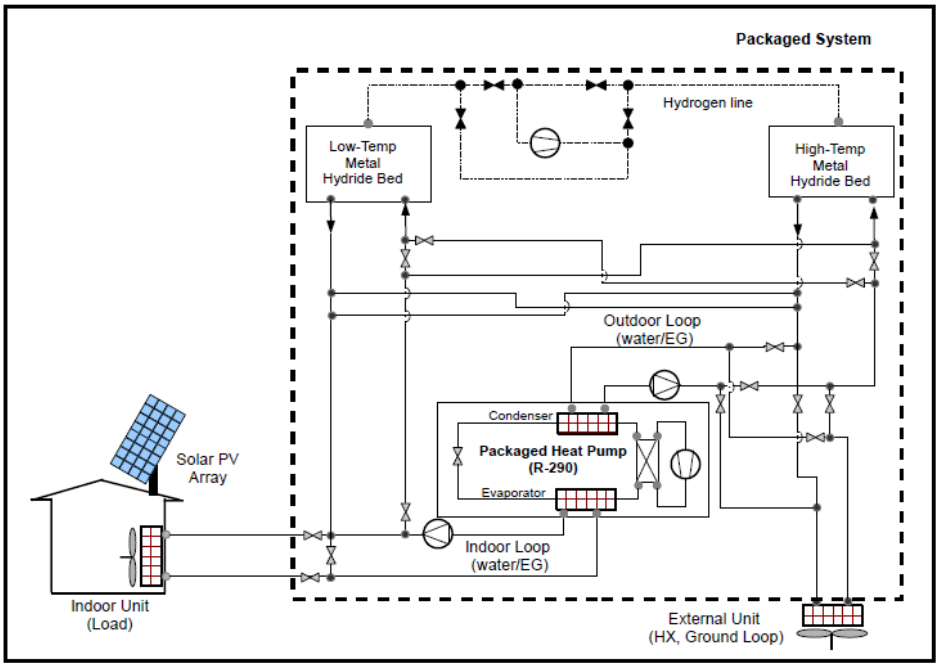

Figure 1: Schematic of the system for residential heating and cooling, with energy storage and on-site solar PV, including solar PV array, packaged heat pump, secondary loops, house, external unit, hydride reactors, and hydrogen line between the reactors. The condenser and evaporator in the packaged heat pump are labelled as in cooling mode; in heating mode they are reversed.

A model of this system, which is used to determine the cost savings from using metal hydride energy storage, is described in Krane *et al.* (2021). The system modelled in this paper differs from that system due to the addition of solar PV to the system. The model includes a sub-model that calculates the power generated by the solar PV based on available solar radiation data, described in Section 2.2. In addition, the load-shifting control logic used in the static model is modified in order to make maximum use of available solar power, as described in Section 2.3.

2.2 Solar Generation Model

In order to incorporate solar power generation into the model, it is necessary to calculate the solar power generation from the solar radiation data for a particular time. The solar power generation, $\dot{W}_{solar}$, is calculated from

$$\dot{W}_{solar} = \eta_{PV} A_{PV} I_T. \tag{1}$$

The efficiency of each solar panel, η_{PV}, is assumed to be 20% based on values for existing models, and the surface area, A_{PV}, of the solar array is determined as described section 3.1. The incident radiation on the solar panel, I_T, is calculated using the following equation (Tina *et al.*, 2006).

$$I_T = \left(R_b + \frac{1-\cos\beta}{2}\rho\right) GHI + \left(\frac{1+\cos\beta}{2} - R_b\right) DHI. \tag{2}$$

Incident radiation is calculated in terms of the global horizontal incidence, GHI (the solar radiation incident on a horizontal surface), and the diffuse horizontal incidence, DHI. The term for GHI also includes a term for radiation reflected from the ground, calculated in terms of the reflectance of the ground, ρ. A value of 0.2 is assumed for the ground reflectance. The slope of the solar panel, β, is 30°. The ratio of beam radiation on the surface to horizontal radiation, R_b, is calculated for south-facing solar panels at the given slope using equations given in Duffie, Beckman, and McGowan (2013). Hourly temperature data for the location is used for GHI and DHI.

2.3 Load-shifting Control Logic

The control logic used to determine whether the energy storage system will be charged or discharged, and what the load on the storage system will be, is shown in Figure 2. At the beginning of each day, the model calculates the average loads on the heat pump for charging and discharging by assuming that the system will be fully charged during off-peak hours and fully discharged during on-peak hours. Thus, the heat pump load for charging during off-peak periods is calculated by adding the total load required by the house during this period to the load required to charge the storage system and averaging this total load over the full time period to find the load on the heat pump throughout the charging people. The heat pump load for the on-period is calculated similarly, except that the load is reduced by the storage capacity of the storage system instead of being increased by it.

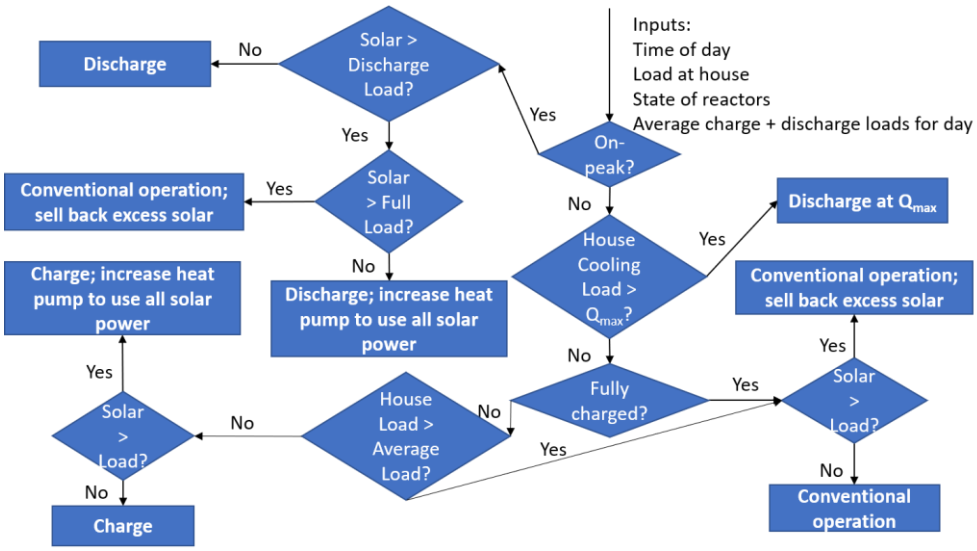

Figure 2: Diagram of the control logic used to modify the load at the heat pump based on available solar power.

At each time step, the control logic first checks if this time is an on-peak or off-peak hour for the TOU rate structure. If it is on-peak, it next compares the available solar power to the average discharge load to see if this load should be used or if the load on the heat pump should be higher in order to make use of excess solar generation. If the system requires electricity from the grid to run the heat pump at the average load, it will run at the average load. But if there is excess solar power available, the heat pump load will be increased to use all of this solar power (and the load on the energy storage system will be decreased by the same amount). If there is enough solar power to provide the entire heating or cooling load without using energy storage, then the system will do so, running in conventional mode with no discharging or charging of the reactors.

During on-peak hours, the system is still discharged in cooling mode if this is necessary due to the load at the house exceeding the capacity of the heat pump (in heating mode, auxiliary heating is used to make up the difference, and not energy storage). If this is not the case, the energy storage system will be charged if it is not already fully charged and if the required heating or cooling load at the house does not exceed the average heat pump load for charging. When charging, the heat pump will run at the average load calculated for charging, unless doing so would not use all available solar power. In that case, the load on the heat pump is increased (and thus, a greater heating or cooling load is delivered to charge the hydride reactors) to either use all available solar power or, if the load that would use all available solar power exceeds the capacity of the heat pump, run the heat pump at maximum capacity. If the system is not charging, due to already being fully charged or the required load at the house being too large, then the system will run conventionally (no charging or discharging of the reactors), with any excess solar power being sold back to the grid.

2.4 Utility Rate Structures

Significant solar penetration is likely to lead to peak demand for electricity from the grid occurring in the morning and evening instead of the afternoon. The utility rate structures that are used to examine the performance of the metal hydride storage system have on-peak periods selected based on this. Therefore, three different on-peak schedules are examined, as shown in Table 1: one with on-peak rates in the morning, one with on-peak rates in the evening, and one with on-peak rates in both morning and evening.

Table 1: On-peak periods examined as the basis for TOU utility rate structures. All on-peak periods are only on weekdays (Monday-Friday); rates are always off-peak on weekends.

	Morning	Evening	Morning and Evening
On-Peak Period	6-11 AM	7-11 PM	6-11 AM & 7-10 PM

For each of these three on-peak periods, a series of rate structures are analyzed. Different potential rate structures are evaluated by varying the ratio of the on-peak to off-peak rates to see how strongly the rates must incentivize load-shifting for the system to be economical. Moreover, each rate structure is compared to an equivalent structure that uses an on-peak demand charge instead of a higher on-peak utility rate. In both cases, all rate structures are defined so that they result in the same annual operating cost for a system with no energy storage (but with solar power generation). Any difference in operating costs between two such rate structures is therefore due to the effect of the energy storage system.

All rate structures studied were defined to have the same total annual operating cost as a conventional system (with solar PV and no energy storage) with a flat utility rate of $0.12/kWh. The rate structures defined in this way for the case with morning and evening peak periods are shown in Table 2. Note that for the cases with only morning or only evening peak periods, the rate structures will have different on-peak and off-peak rates for the same on-peak to off-peak ratio, since achieving the same annual operating cost for the conventional system requires different rates depending on the length of the on-peak period.

Table 2: Rate structures used for the case with morning and evening on-peak periods. Rate structures with a high on-peak rate are defined by the on-peak to off-peak rate ratio. Each rate structure with a flat rate and an on-peak demand charge is defined to be equivalent to a structure with a high on-peak rate by having the same percentage of the operating costs for a conventional system occur in the on-peak period and having the flat rate equal the off-peak rate for the structure with a high on-peak rate.

		High On-Peak Rates				On-Peak Demand Charge			
		Summer		Winter		Summer		Winter	
% Conv. Cost On-Peak	On-peak/ Off-peak Ratio	On-peak Rate (/kWh)	Off-peak Rate (/kWh)	On-peak Rate (/kWh)	Off-peak Rate (/kWh)	Flat Rate (/kWh)	On-peak Demand Charge (/kW)	Flat Rate (/kWh)	On-peak Demand Charge (/kW)
35.5	1	$0.1200	$0.1200	$0.1200	$0.1200	$0.1200	$0.00	$0.1200	$0.00
52.3	2	$0.1729	$0.0864	$0.1791	$0.0895	$0.0864	$6.48	$0.0895	$5.90
68.7	4	$0.2217	$0.0554	$0.2376	$0.0594	$0.0554	$12.47	$0.0594	$11.74
73.3	5	$0.2350	$0.0470	$0.2542	$0.0508	$0.0470	$14.10	$0.0508	$13.40
76.7	6	$0.2447	$0.0408	$0.2666	$0.0444	$0.0408	$15.30	$0.0444	$14.64
81.4	8	$0.2582	$0.0323	$0.2840	$0.0355	$0.0323	$16.95	$0.0355	$16.37
84.6	10	$0.2669	$0.0267	$0.2955	$0.0296	$0.0267	$18.02	$0.0296	$17.52
89.1	15	$0.2796	$0.0186	$0.3125	$0.0208	$0.0186	$19.58	$0.0208	$19.21

There are two sets of rate structures shown in Table 2; one set uses TOU rates with a higher rate during the on-peak period, while the other uses a flat rate with an on-peak demand charge. Rate structures in the first set are defined by the ratio of the on-peak rate to the off-peak rate. As this ratio increases, a higher percentage of the operating cost for the conventional system occurs during the on-peak period and there is thus a greater opportunity for cost savings with energy storage. Each rate structure with an on-peak demand charge is defined so that it has the same percentage of the total operating cost occur during the on-peak period as one of the structures with TOU rates, and also uses the off-peak rate from that structure as its flat rate. By comparing these two rates with the same percentage of the conventional operating cost during on-peak hours, we can see which of on-peak demand charges and high on-peak rates results in larger cost savings from the use of energy storage.

3. RESULTS

3.1 Component Sizing and Initial Cost Calculations

The conventional system consists of a heat pump, used to deliver both heating and cooling loads to the house, and auxiliary electric heating used to supplement the heat pump if the heating load at the house exceeds its capacity. The system with energy storage adds contains both of these components, but also adds two secondary loops with pumps and internal and external air-handling units (the indoor and outdoor loops), two metal hydride reactors, and a compressor used to move hydrogen between the reactors. $LaNi_5$ is used as the metal hydride in one reactor, and $MmNi_{4.5}Cr_{0.5}$ in the other. The initial cost of each system is the sum of the costs of all of its components.

An estimated cost of $10/kW capacity is used for the auxiliary electric heating by examining the prices and maximum capacities of commercially-available units. For the residential heat pump considered in this case study, the cost, y_{hp}, is estimated as a function of the rated capacity (Q_{rated}) and SEER, based on a correlation developed by the Energy Efficiency and Renewable Energy Office (Energy Efficiency and Renewable Energy Office, 2016):

$$y_{hp} = 1.91 * 10^3 - 41.4SEER_{rated} + 7.48{SEER_{rated}}^2 + 589Q_{rated} - 16.4{Q_{rated}}^2 \quad (3)$$

The most expensive component in the energy storage system is the metal hydride reactors. The reactor cost is determined by estimating the material costs for the hydrides, since this is much higher than the installation or material costs for the heat exchanger. An estimated price of $20/kg is used for $LaNi_5$, based on examining existing products. Since similar information was not available for $MmNi_{4.5}Cr_{0.5}$, a cost of $24/kg is estimated based on comparing raw material prices for lanthanum and mischmetal ("Argus Rare Earths Monthly Outlook," 2017). Both of these costs are reduced by 25% to account for the gains from recycling them at the end of their life cycle, so the actual values used are $15/kg for $LaNi_5$, and $18/kg for $NdNi_{4.8}Sn_{0.2}$. The total cost of piping for an indoor secondary loop for a typical residence, including pump and air-handling unit, was estimated by Tam *et al.* to be $1301 (2018). Based on a cost breakdown for a secondary-loop system, the cost of the outdoor secondary loop, where the indoor air-handling system is replaced with an outdoor heat exchanger, is estimated to be $1050. Since hydrogen compressors are usually used at much larger pressure ratios than the 10-bar limit imposed in this case, the cost of the compressor is estimated by comparing prices for air compressors with the appropriate operating pressures, resulting in an estimate value of $200.

Table 3: Cost comparison between the conventional HVAC system and the system with metal hydride energy storage. Both systems also include solar PV used for power generation, which is used by the HVAC system as well as other electrical systems in the house.

System	Initial Cost						
	Heat Pump	**Electric Heating**	**Hydrogen Compressor**	**Secondary Loops**	**Metal Hydrides**	**Solar PV**	**Total**
Conventional	$5096	$100	-	-	-	$12,600	$17,796
Energy Storage	$5096	$120	$200	$2351	$14,610	$12,600	$34,977

A 3-ton heat pump is assumed for both the conventional system and the system with energy storage. This heat pump is sized to meet the maximum cooling load; it is not downsized for the system with storage because doing so would significantly increase operating costs due to a greater reliance on auxiliary heating in the winter. The hydride reactors are sized to have sufficient storage capacity to flatten the cooling load for the heat pump on the hottest day of the year. To ensure that the control logic for using excess solar power generation would be used, the solar panels are sized to a summer design day such that peak generation on that day exceeds power consumption at that time. This results in a total surface area of 21 m^2 for the solar panels for the case study considered. A price of $600/$m^2$ is used to calculate the total price of the solar panels, based on costs for existing systems. It should be noted that since the heat pump and solar panels are the same size for the systems with and without storage, their costs have no effect on the difference in cost between the systems (and therefore no effect on the payback period).

3.2 System Behavior on an Example Day

To show how the control logic for using energy storage for load shifting and making the best use of available solar power works on a particular day, the model is run using temperature and solar irradiation data for June 23 from the Typical Meteorological Year 3 (TMY3) data for Elizabeth City, NC (NREL, n.d.). The hourly non-HVAC electricity loads are estimated using data from the Office of Energy Efficiency & Renewable Energy (EERE) on residential

hourly electricity loads (EERE, n.d.). We selected a city in the American South as the object of this study because it is the only region in the United States where electric heating, as is used in our system, is more commonly used than gas heating (Comstock, 2014).

The results for this example day can be seen in Figure 3 . The storage system is partially discharged during each on-peak period, as seen in Figure 3b. While discharging, the heat pump is run at a low load, as seen in Figure 3a. However, for the last hour of the first on-peak period, the storage system is not used even though there is a cooling load larger than the load the heat pump had previously run at during this on-peak period. This is because there is enough solar power available at this time that all of the cooling load can be met with the heat pump without using any electricity from the grid. Since this is the case, the storage system is not used at this time to reduce the load on the heat pump.

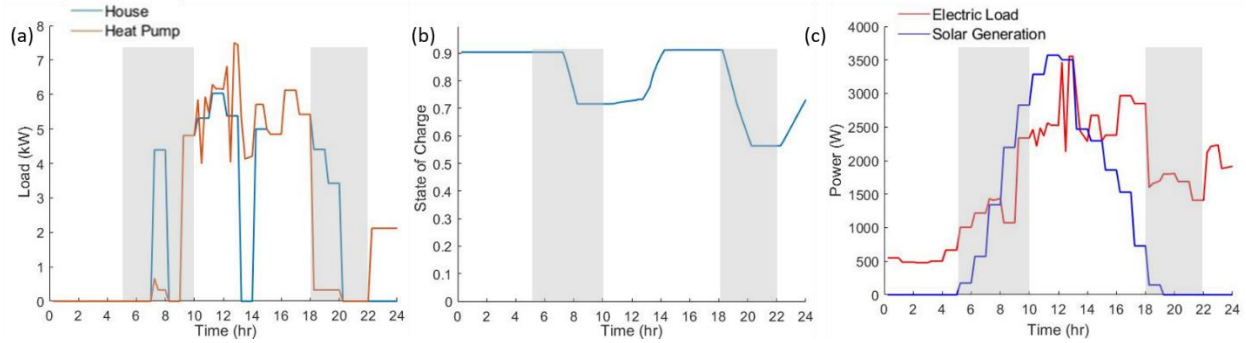

Figure 3: (a) Cooling loads at the house and heat pump, (b) reactor state of charge, and (c) total electric load for the house compared to solar power generation for an example summer day in Elizabeth City, NC. On-peak periods are highlighted in grey.

If no excess solar power were available, the system would not be charged in between the morning and evening on-peak periods, since the heat pump loads for discharging are calculated so that the system will be fully discharged by the combination of the two periods, and then charged during off-peak hours at night, when the cooling load is lower. However, in this case, solar power generation during the afternoon on-peak period exceeds the power needed at the house, as seen in Figure 3c, so the excess solar power is sued to charge the storage system. While charging, the heat pump load exceeds the cooling load at the house, and the excess is used to charge the storage system. However, at two points during the afternoon the heat pump load goes below the cooling load at the house. This is because the system is adjusting the temperatures in the metal hydride reactors in order to keep them within the range of temperatures the system is designed to operate in. When this happens, some of the cooling load is being provided by the hydride reactors, because the fluid in the indoor loop is being used to heat the hydride reactor connected to it. The system is also charged during the night after the end of the evening on-peak period. This charging is done at a constant heat pump load since it is using electricity from the grid and thus not trying to adjust the load in order to only use solar power.

3.3 Cost Savings and Payback Period

Using the system sized as described in Section 3.1, the model is run for a full year for a house in Elizabeth City, NC. TMY3 weather data (NREL, n.d.) and EERE data on non-HVAC building loads (EERE, n.d.) for the full year are used as described in the previous section. The annual operating cost calculated for the conventional system (with solar PV but no energy storage) is $1422.18. This cost is the same for all rate structures since these are defined to give the same annual operating cost if no storage is used. The majority of the operating cost is due to electrical loads other than the HVAC system, which has an operating cost of $622.33 for the flat rate of $0.12/kWh. The operating cost savings for all the rate structures considered are shown in Figure 4. Cost savings are plotted against the percentage of the conventional system operating costs that occur during the on-peak period. The higher this value is, the larger the incentive to use energy storage. For each of the three on-peak periods considered (morning, evening, and morning and evening) rates with a high on-peak rate are compared to rates with a constant electricity rate and an on-peak demand charge.

As illustrated in Figure 4, the cost savings increase with rate structures where conventional systems have increasing fraction of the costs during the on-peak period. Further, these cost savings are greater for rate structures with an on-

peak demand charge than rate structures with only high on-peak rates. Both trends are also observed regardless of the designated on-peak times (morning, evening, or both). The largest cost savings occur for rates with a morning on-peak period, and the smallest cost savings for rates with morning and evening on-peak periods, with the maximum savings for the rates examined being less than half the maximum for rates with morning on-peak periods.

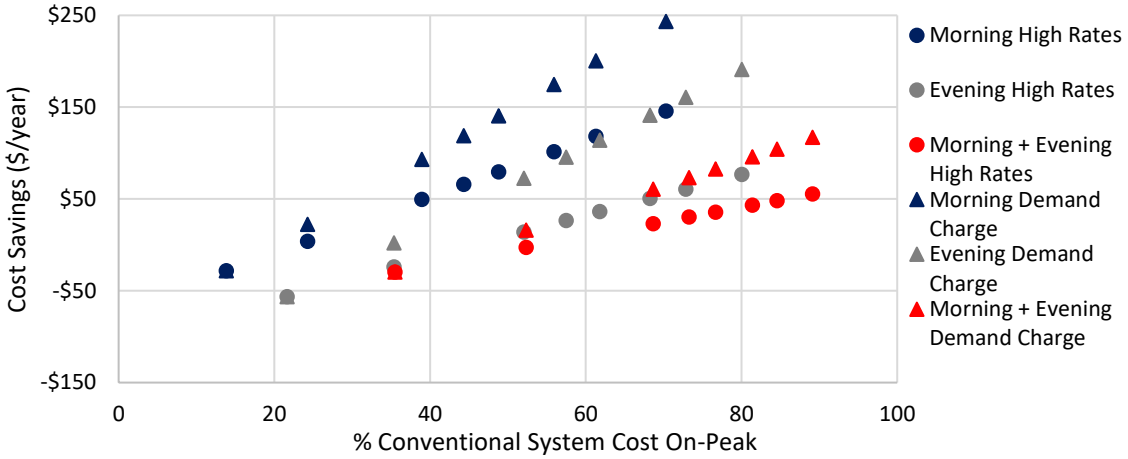

Figure 4: Annual cost savings for all TOU rates structures considered in this study, plotted as a function of the percentage of the conventional system operating cost that occurs during the on-peak period. Rates with high on-peak rates are compared to rates with an on-peak demand charge for rate structures with three different on-peak times (morning, evening, and morning and evening). Within each of these categories, a series of rates are considered to see how cost savings increase as a larger portion of the operating costs occur during the on-peak period due to higher on-peak rates or demand charges. The leftmost point in each series is a flat rate structure with no demand charge.

The higher cost savings for rate structures with demand charges show that the storage system is more successful in reducing the peak power during the on-peak period than it is at reducing the total on-peak energy consumption. This success in reducing peak power is due to the use of a constant heat pump load when discharging (except when a larger load could be used using only solar power), which means that the most energy storage will be used during on-peak hours with peak loads, resulting in a greater reduction in peak power consumption than in total on-peak power consumption. As expected, cost savings increase as the ratio of on-peak to off-peak rates increases, since increasing this ratio increases the cost incentive to shift loads to off-peak. Without any difference between on-peak and off-peak rates, the use of energy storage leads to an increased operating cost, since the total electrical consumption increases due to inefficiencies associated with charging and discharging storage and the use of an additional hydrogen compressor. These penalties outweigh any benefits associated with increased operation of the heat pump at more favorable outdoor temperatures.

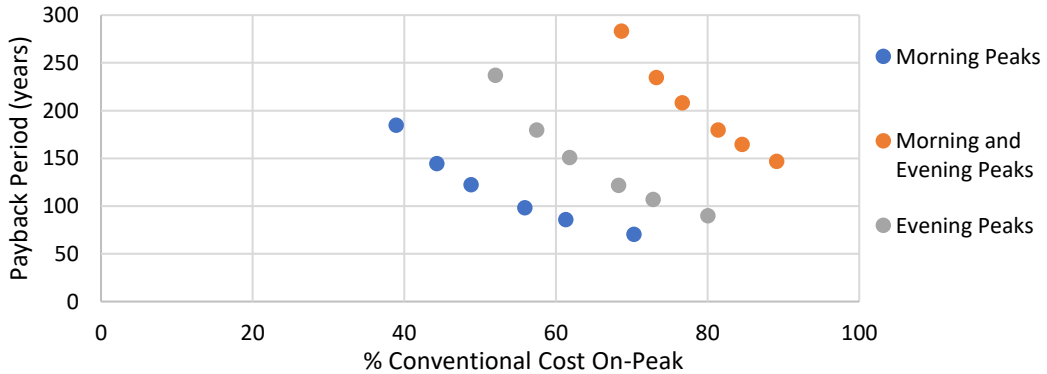

Figure 5: Payback periods calculated based on cost savings from different rate structure, plotted as a function of the percentage of the operating cost that occurs during the on-peak period for a conventional system. Payback period is calculated for the rate with an equivalent demand charge rather than rates with a higher on-peak rate, due to higher cost savings from rates with demand charges.

Estimated payback periods for the system with storage are presented in Figure 5 as function of the utility rates. While the system provides significant cost savings, the resulting payback periods are extremely long and not economically viable, even for the most favorable rate structures. These high payback periods are primarily due to the extremely high cost of the metal hydrides. The increased cost from the two secondary loops is also a significant factor; only at the most favorable rates are the cost savings large enough to pay off the cost of these loops in less than ten years.

4. CONCLUSION

The availability of on-site solar PV increases the benefits associated with energy storage for heating and cooling in residential applications that have time-varying electricity rates. This combination leads to greater utilization of on-site generated electricity. Increased penetration of solar PV will likely improve the benefits as on-peak periods shift and change TOU rate structures to discourage selling of excess electricity back to the grid. Metal hydrides are a potential method for energy storage that can be used for both heating and cooling, thus enabling year-round utilization. This paper investigated the combination of metal hydride storage coupled to a heat pump with onsite solar PV generation as a system that could meet both heating and cooling loads while reducing operating costs compared to a system with just solar PV. The performance of this system was investigated assuming utility rates that might be representative of a scenario with high levels of solar penetration on the grid. However, the cost savings are not large enough to result in a viable payback period even with very favorable rate structures. Rates with morning on-peak periods resulted in the largest cost savings, followed by rates with evening on-peak periods; both resulted in larger savings than rates with on-peak periods in both the morning and the evening. For all on-peak periods studied, rate structures with on-peak demand charges resulted in larger cost savings than rate structures where the electricity rate was higher during the on-peak period.

REFERENCES

Abji, N., Tizghadam, A., & Leon-Garcia, A. (2015). Energy storage management in core networks with renewable energy in time-of-use pricing environments. *IEEE International Conference on Communications*, *2015-Septe*, 135–141. https://doi.org/10.1109/ICC.2015.7248311

Argus Rare Earths Monthly Outlook. (2017). *Argus Consulting Services*, (17–9).

Comstock, O. (2014). Everywhere but Northeast, fewer homes choose natural gas as heating fuel. Retrieved from Today in Energy website: https://www.eia.gov/todayinenergy/detail.php?id=18131

Corgnale, C., Hardy, B., Motyka, T., & Zidan, R. (2016). Metal hydride based thermal energy storage system requirements for high performance concentrating solar power plants. *International Journal of Hydrogen Energy*, *41*(44), 20217–20230. https://doi.org/10.1016/j.ijhydene.2016.09.108

Duffie, J. A., Beckman, W. A., & McGowan, J. (2013). Solar Engineering of Thermal Processes. In *American Journal of Physics* (Vol. 53). https://doi.org/10.1119/1.14178

EERE. (n.d.). Commercial and Residential Hourly Load Profiles for all TMY3 Locations in the United States. Retrieved from OpenEI website: https://openei.org/doe-opendata/dataset/commercial-and-residential-hourly-load-profiles-for-all-tmy3-locations-in-the-united-states

Energy Efficiency and Renewable Energy Office. (2016). Technical support document: Energy efficiency program for consumer products: Residential central air conditioners, heat pumps, and furnaces. *US Department of Energy*, (December).

Feng, P., Zhu, L., Zhang, Y., Yang, F., Wu, Z., & Zhang, Z. (2018). Optimum output temperature setting and an improved bed structure of metal hydride hydrogen storage reactor for thermal energy storage. *International Journal of Hydrogen Energy*, 1–13. https://doi.org/10.1016/j.ijhydene.2018.04.220

Hasnain, S. M. (1998). Review on sustainable thermal energy storage technologies, part II: Cool thermal storage. *Energy Conversion and Management*, *39*(11), 1139–1153. https://doi.org/10.1016/S0196-8904(98)00024-7

Henze, G. P. (2003). An Overview of Optimal Control for Central Cooling Plants with Ice Thermal Energy Storage.

Journal of Solar Energy Engineering, *125*(3), 302–309. https://doi.org/10.1115/1.1591801

Janko, S. A., Arnold, M. R., & Johnson, N. G. (2016). Implications of high-penetration renewables for ratepayers and utilities in the residential solar photovoltaic (PV) market. *Applied Energy*, *180*, 37–51. https://doi.org/10.1016/j.apenergy.2016.07.041

Krane, P., Ziviani, D., Marconnet, A., Braun, J., & Jain, N. (2021). Metal-Hydride Energy Storage to Enable Load-Shifting for Heat Pumps in Heating and Cooling Modes for Buildings. *To Be Submitted to Energy & Buildings*.

Leger, A. S., Sobiesk, E., Farmer, A., & Rulison, B. (2014). Demand response with photovoltaic energy source and time-of-use pricing. *Proceedings of the IEEE Power Engineering Society Transmission and Distribution Conference*, 1–5. https://doi.org/10.1109/tdc.2014.6863304

Myers, K. S., Klein, S. A., & Reindl, D. T. (2010). Assessment of high penetration of solar photovoltaics in Wisconsin. *Energy Policy*, *38*(11), 7338–7345. https://doi.org/10.1016/j.enpol.2010.08.008

Nassif, N., Tesiero, R. C., & Singh, H. (2013). Impact of Ice Thermal Storage on Cooling Energy Cost for Commercial HVAC Systems. *ASHRAE Transactions*, *119*.

NREL. (n.d.). 1991-2005 Update: Typical Meteorlogican Year 3. Retrieved from National Solar Radiation Database website: https://rredc.nrel.gov/solar/old_data/nsrdb/1991-2005/tmy3/

Nyamsi, S. N., Lototskyy, M., & Tolj, I. (2018). Selection of metal hydrides-based thermal energy storage: Energy storage efficiency and density targets. *International Journal of Hydrogen Energy*, *43*(50), 22568–22583. https://doi.org/10.1016/j.ijhydene.2018.10.100

Sanaye, S., & Shirazi, A. (2013). Thermo-economic optimization of an ice thermal energy storage system for air-conditioning applications. *Energy and Buildings*, *60*, 100–109. https://doi.org/10.1016/j.enbuild.2012.12.040

Sheppard, D. A., Paskevicius, M., Humphries, T. D., Felderhoff, M., Capurso, G., Bellosta von Colbe, J., … Buckley, C. E. (2016). Metal hydrides for concentrating solar thermal power energy storage. *Applied Physics A: Materials Science and Processing*, *122*(4). https://doi.org/10.1007/s00339-016-9825-0

Tam, A., Braun, J. E., Ziviani, D., & Jain, N. (2018). An Overall Assessment of Ice Storage Systems for Residential Buildings. *5th International High Performance Buildings Conference at Purdue*, (July).

Tam, A., Ziviani, D., Braun, J. E., & Jain, N. (2019). Development and evaluation of a generalized rule-based control strategy for residential ice storage systems. *Energy & Buildings*, *197*, 99–111. https://doi.org/10.1016/j.enbuild.2019.05.040

Tina, G., Gagliano, S., & Raiti, S. (2006). Hybrid solar/wind power system probabilistic modelling for long-term performance assessment. *Solar Energy*, *80*(5), 578–588. https://doi.org/10.1016/j.solener.2005.03.013

VanGeet, O., Brown, E., Blair, T., & McAllister, A. (2008). Solar San Diego: The impact of binomial rate structures on real PV-systems. *American Solar Energy Society - SOLAR 2008, Including Proc. of 37th ASES Annual Conf., 33rd National Passive Solar Conf., 3rd Renewable Energy Policy and Marketing Conf.: Catch the Clean Energy Wave*, *6*, 3819–3844.

Voskuilen, T. G., Waters, E. L., & Pourpoint, T. L. (2014). A comprehensive approach for alloy selection in metal hydride thermal systems. *International Journal of Hydrogen Energy*, *39*(25), 13240–13254. https://doi.org/10.1016/j.ijhydene.2014.06.119

Ward, P. A., Corgnale, C., Teprovich, J. A., Motyka, T., Hardy, B., Sheppard, D., … Zidan, R. (2016). Technical challenges and future direction for high-efficiency metal hydride thermal energy storage systems. *Applied Physics A: Materials Science and Processing*, *122*(4). https://doi.org/10.1007/s00339-016-9909-x